JOURNAL OF GEOPHYSICAL RESEARCH, VOL. 111, A08102, doi:10.1029/2005JA011459, 2006

Click Here for Full Article

Galactic cosmic ray flux decline and periodicities in the interplanetary space during the last 3 centuries revealed by ^{44}Ti in meteorites

C. Taricco,[1,2] N. Bhandari,[3] D. Cane,[1,2] P. Colombetti,[1,2] and N. Verma[1,2]

Received 5 October 2005; revised 7 February 2006; accepted 30 March 2006; published 4 August 2006.

[1] ^{44}Ti and ^{26}Al activities and heavy nuclei tracks produced by cosmic rays have been measured in 19 stone meteorites that fell during the period 1766 to 2001. The gamma activity measurements of cosmogenic isotopes were performed using a highly specific and selective large volume Ge-NaI (Tl) spectrometer. The ^{44}Ti activity, corrected for the target element abundances and shielding effects, shows a decrease of about 43% over the past 235 years. Superimposed on this declining trend, the ^{44}Ti activity shows a centennial oscillation. The variations in ^{44}Ti activity are related to changes in cosmic ray intensity caused by heliospheric magnetic field modulation in the interplanetary space between heliocentric distances of 1 and 3 AU. Using the relations between solar open magnetic flux, modulation parameter, and galactic cosmic ray flux, we have calculated the variation in production rates of ^{44}Ti in meteorites back to about 1700 AD. We show that the measured ^{44}Ti activity in meteorites over the past 235 years and the calculated production rates are in agreement. Our results are consistent in phase and magnitude with doubling of the solar open magnetic field intensity over the past century. The data also imply that the centennial scale oscillation deduced by ^{44}Ti is in phase with Gleissberg solar cycle, but its amplitude is larger than expected from the calculated cosmic ray flux.

Citation: Taricco, C., N. Bhandari, D. Cane, P. Colombetti, and N. Verma (2006), Galactic cosmic ray flux decline and periodicities in the interplanetary space during the last 3 centuries revealed by ^{44}Ti in meteorites, *J. Geophys. Res.*, *111*, A08102, doi:10.1029/2005JA011459.

1. Introduction

[2] The interdependence between solar activity, solar magnetic field, solar irradiance, cosmic ray intensity, and terrestrial climate and their variability with time is a subject of intense debate and study. The solar activity shows variability on many timescales, the best known among them is the 11-year Schwabe cycle. The sunspot number (R) and the geomagnetic indices (e.g., aa, Kp, and aurorae) are some of the parameters defined to characterize solar magnetic activity and its terrestrial effects and allow us to estimate its variation in the past. Recent measurements of total solar irradiance (S) in space, with the surprising finding that the Sun is brighter at sunspot maximum, provide the possibility of investigating the long-debated problem of the bolometric impact of solar activity on climate, either directly or via complex amplification mechanisms. The relation among total magnetic flux and the open magnetic flux (f_0) responsible for the Interplanetary Magnetic Field (IMF) and solar irradiance is at present a crucial issue [*Lean et al.*, 2002].

[3] The heliospheric magnetic field modulates the Galactic Cosmic Ray (GCR) intensity which has been measured by ground-based neutron monitors and balloon- and spacecraft-borne measurements at top of the atmosphere or in the interplanetary space. On the basis of these measurements, the shape of GCR energy spectrum is defined by solar modulation parameter, Φ, as a function of the phase of the solar cycle. The influence of interplanetary medium in modulating the GCR flux was shown many years ago by the measurement of the differential energy spectrum of hydrogen and helium nuclei as a function of the phase of the 11-year solar cycle [see, e.g., *Webber and Yushak*, 1979] from balloon-borne observations and from measurements in space by IMP 3 and IMP 5. The modulation of GCR as a function of position, energy, and time in the heliosphere is a complex combination of several mechanisms. *Bieber et al.* [1993], using the yearly averaged data, have noted that the GCR density and the interplanetary magnetic field IMF at 1 AU are anticorrelated. This has also been shown to hold in the outer heliosphere by *Burlaga et al.* [1993]. It was suggested [*Cane et al.*, 1999; *Belov*, 2000; *Rouillard and Lockwood*, 2004] that there is a close anticorrelation between GCR and the IMF intensity, both for the long-term gradual changes and the sudden step-like changes. Models of inward transport of GCR have been successfully developed in the last 30 years [*Axford*, 1972; *Jokipii*, 1991; *Potgieter*, 1993; *Potgieter et al.*, 2001]. However, owing to complexity of the modulation dynamics, they do not allow a simple description of GCR spectrum in the inner

[1]Dipartimento di Fisica Generale, Università di Torino, Torino, Italy.
[2]Also at Istituto di Fisica dello Spazio Interplanetario (IFSI), Istituto Nazionale di Astrofisica, Torino, Italy.
[3]Physical Research Laboratory and Basic Sciences Research Institute, Navrangpura, Ahmedabad, India.

Copyright 2006 by the American Geophysical Union.
0148-0227/06/2005JA011459$09.00

heliosphere as a function of the phase of the solar cycle. *Castagnoli and Lal* [1980] examined the changes in the GCR flux with the solar cycle in the past and, guided by the observations during cycles 17 to 20, using the force field approximation solution of the transport equation [*Urch and Gleason*, 1972] gave an empirical formula for differential transport of proton flux (>100 MeV), J_G (particles per m^2 sr MeV), in terms of a single modulation parameter Φ (MeV), which turns out to be characteristic of different phases of the solar cycle.

[4] The spectra of primary cosmic rays have been obtained from balloon and spacecraft measurements during different phases of the solar cycles 20 to 23; the Climax neutron monitor time series is available since 1953 [*Hsieh et al.*, 1971]; the annual mean of the coronal source magnetic flux as derived from the aa index is available since 1868 and the sunspot number time series from 1600 AD [*Waldmeier*, 1961].

2. Variation of Heliospheric Magnetic Field in the Past

[5] The magnitude of variations in solar activity indices within a solar cycle and over long periods of time are currently being debated because of their effect on terrestrial climate. *Lockwood et al.* [1999], on the basis of the analysis of the geomagnetic index aa, showed that the Sun's coronal source magnetic flux has risen by a factor of 1.4 since 1964 and doubled during the past 100 years. *Solanki et al.* [2000] reproduced this increase from their model of the open solar magnetic flux f_0 which determines the radial interplanetary magnetic field component. Whereas the irradiance changes on short timescales depend on sunspots and the active region faculae, the long-term changes depend on magnetic network [*Lean*, 2000]. Since the irradiance has severe consequences on terrestrial climate, it is important to understand the heliospheric magnetic field variations, particularly the long-term changes. The behavior of the Sun during prolonged quiet times like the Spörer (1416–1534) and Maunder minima (1645–1715) is also a point of debate. Some studies show that the GCR spectrum in the interplanetary space during Maunder minimum was like the local interstellar space [*Webber and Lockwood*, 2001].

[6] *Stozhkov et al.* [2000] used the stratospheric balloon data and neutron monitor and ionization chamber ground data to determine the cosmic ray flux during four consecutive solar minima (1964–1965, 1976–1977, 1987–1988, 1996–1997) and concluded that there is a negative trend (0.01–0.09% per year) in cosmic ray flux. They also found that this can only be explained if cosmic rays were produced by a nearby (30–150 parsec) supernova explosion, 10^4 to 10^5 years ago. Other than the solar modulation, the proposed supernova thus added one more mechanism for cosmic ray variation in the interplanetary space. In another paper, *Stozhkov et al.* [2001] concluded that since 1937, the magnetic flux from the Sun in the heliosphere, smoothed over 11 year period, did not increase and this result is in contradiction to the work of *Lockwood et al.* [1999]. *Ahluwalia and Lopate* [2001] has refuted the supernova hypothesis, preferring the convective removal of GCR by solar wind to be the reason for the cosmic ray modulation.

[7] The solar magnetic field modulates the galactic cosmic ray flux and hence one approach to determine the cosmic ray flux in the past is to study cosmogenic isotopic records. Measurements of isotopes, e.g., ^{10}Be and ^{14}C produced in the atmosphere and deposited in sediments or ice cores or incorporated in other terrestrial reservoirs like trees have been made which provide long time series. The 88–90 year periodicity in ^{14}C spectrum is possibly related to the Gleissberg cycle [*Gleissberg*, 1967; *Cohen and Lintz*, 1974; *Stuiver and Quay*, 1980] which envelops the 11- year Schwabe cycles [*Damon and Sonett*, 1991]. On the basis of these measurements, some long-term periodicities (e.g., ~200-year Suess wiggles) have also been found in tree rings, sea sediments [*Castagnoli et al.*, 1998], and ice cores from Greenland and Antarctica. However, ^{10}Be and ^{14}C concentrations are also affected by terrestrial phenomena such as geomagnetic field, climatic changes, deposition rate variations, and exchange within the various terrestrial reservoirs, all of which tend to mask the solar signal. Therefore it is difficult to quantify and separate the variations in nuclide production rates due to cosmic rays and the climatic influence in the terrestrial records. In view of the above discussion it appears desirable to have a reliable and independent index which records the cosmic ray flux in the interplanetary space and is not influenced by terrestrial processes. Cosmogenic isotopes in meteorites, which are produced when the rocks are exposed to cosmic rays in the interplanetary space, offer a unique tool for decoupling the terrestrial causes from the solar activity variations. In particular, we have identified ^{44}Ti (half-life 59.2 years) as an ideal index in meteorites, useful for studying GCR variations on centennial scale, free from interference due to terrestrial processes [*Bonino et al.*, 1995].

3. Cosmogenic Isotopes in Meteorites

[8] Cosmic rays produce a large number of radioactive and stable isotopes in meteorites as they travel through the interplanetary space before falling on the Earth. About 20 radioisotopes, such as ^{46}Sc, ^{22}Na, ^{14}C, ^{44}Ti, ^{39}Ar, and ^{26}Al, having mean life ranging between days to millions of years, have been measured in several stony meteorites [see, e.g., *Honda and Arnold*, 1960; *Bhandari et al.*, 1988]. Their production rates and depth profiles have been calculated by *Michel et al.* [1991] and in some cases experimentally determined by measuring activities along cores taken from some well documented meteorites [*Bhandari et al.*, 1993]. The production rate (and hence the activity) of a radioisotope in a meteorite depends on the primary cosmic ray intensity in space, roughly over a mean life of the isotope before the meteorite falls on the Earth when the cosmic ray irradiation ceases. Therefore it is possible to study GCR variations on different timescales by measuring radioisotopes having different half lives. However, since the flux of cosmic ray secondaries, because of development of the nuclear cascade, within a meteorite changes with the size (or with radius r, under assumption of spherical approximation of meteoroid shape), and with the shielding depth of the sample (ΔX), the isotope production rate also depends on these shielding parameters (r, ΔX). These can be determined by measuring the density of heavy nuclei tracks in meteoritic minerals, whose production rate is very sensitive to

Table 1. Some Relevant Details of the Meteorites Studied in the Present Work

	Meteorite (Class)	Date of Fall	Recovered Mass, Kg	Fe + Ni, %	K,[b] ppm	^{21}Ne Exposure Age, Ma	Source of Meteorite[a]
1	Albareto (LL4)	July, 1766	~2	20.98	863	38.9	Modena Museum
2	Mooresfort (H5)	Aug, 1810	3.52	28.6 + 1.94	879	10.3	National Museum, Ireland
3	Charsonville (H6)	23.11.1810	27	25.2 + 1.74	777	63.3	NHM, Vienna
4	Agen (H5)	5.9.1814	30	27.45 + 1.74	(785)	7	Vatican Obs. Rome
5	Cereseto (H5)	17.7.1840	6.46	27.45 + 1.75	772	4.5	Museo di scienza naturale, Torino
6	Grüneberg (H4)	22.3.1841	1	26.9 + 1.69	(776)	6.7	MFN, Berlin
7	Kernouve' (H6)	22.5.1869	80	28.39 + 1.7	782	3	NHM Vienna
8	Alfianello (L6)	16.2.1883	228	21.6 + 1.35	859	25.3	Vatican Obs. Rome
9	Bath (H4)	29.8.1892	21.18	26.1 + 1.52	776	7.4	NHM, Vienna
10	Lancon (H6)	20.6.1897	7	27.2 + 1.78	782	6.6	Vatican Obs. Rome
11	Holbrook (L6)	19.7.1912	220	20.5 + 1.08	855	16	Vatican Obs. Rome
12	Olivenza (LL5)	19.6.1924	150	18.9 + 1.05	829	11.6	Vatican Obs. Rome
13	Rio Negro (L4)	21.9.1934	1.31	21.4 + 1.17	830	21.5	Vatican Obs. Rome
14	Monze (L6)	5.10.1950	>5	21.6 + 1.74	890	9.9	Vatican Obs. Rome
15	Dhajala-272 (H3/4)	28.1.1976	75	27.96 + 1.67	820	8.9	PRL, India
16	Torino (H6)	18.5.1988	0.977	26.1 + 1.16	680	68	Alenia, Torino
17	Mbale A,T (L5/6)	14.8.1992	150	22.9	909	26.9	DMS, Denmark
18	Fermo (H3-5)	25.9.1996	10.2	29 + 1.82	660	8.8	Municipio di Fermo
19	Dergaon (H5)	2.3.2001	>12	27.3 + 1.82	340	9.7	Gauhati University

[a]MFN: Museum Für Naturkunde. DMS: Dutch Meteor Society. NHM Naturhistorisches Museum PRL: Physical Research Laboratory.
[b]Values in parentheses are the adopted average meteorite class values from *Kallemeyn et al.* [1989] and *Mason* [1971].

shielding. Corrected for the shielding effects, the activity of various radioisotopes can be directly related to the cosmic ray intensity before the fall of the meteorite.

[9] The activity of short-lived isotopes (<1 year) is related to short-term fluctuations in cosmic ray intensity, while ^{22}Na (half-life 2.6 years) and ^{54}Mn (half-life 312 days) are ideally suited for determining cosmic ray intensity over 11-year Schwabe cycle. The long-lived isotopes, e.g., ^{26}Al (half-life 0.73 My), average the cosmic ray intensity over a million years and their activity is insensitive to decadal or century scale variations in cosmic ray flux.

4. Periodicities in Cosmic Ray Intensity Based on Cosmogenic Isotopes

[10] Several periodicities have been observed in isotopic records in meteorites. The 11-year cycle has been clearly seen in the cosmogenic ^{22}Na and shorter-lived radionuclides (e.g., ^{46}Sc, ^{54}Mn) in meteorites which fell during the past few decades [*Bonino et al.*, 1997; *Evans et al.*, 1982; *Potdar et al.*, 1986; *Bhandari et al.*, 1994]. ^{22}Na and ^{26}Al are produced in similar nuclear reactions within stony meteorites and therefore their production depth profiles are similar. The ratio ^{22}Na/^{26}Al is thus nearly independent of shielding parameters (r, ΔX) and virtually no shielding correction is required. Furthermore, since ^{26}Al activity is not influenced by the 11-year Schwabe cycle, ^{22}Na/^{26}Al is a good measure of cosmic ray variations over decadal scale. On the basis of these records in stone meteorites which fell during the last four solar cycles (19 to 23), it has been found that cosmic ray intensity decreased by nearly 20% from solar minima to solar maxima. The 11-year periodicity in cosmic ray intensity has also been seen in ^{10}Be concentration measured in Greenland ice cores [*Masarik and Beer*, 1999].

[11] We have previously shown a century-scale modulation (Gleissberg cycle), expected on the basis of the sunspot series, in the cosmogenic ^{44}Ti activity measured in meteorites which fell during 1883–1992 [*Bonino et al.*, 1995]. ^{39}Ar ($T_{1/2}$ = 269 years) is also suitable for studying variations on century timescales [*Forman and Schaeffer*, 1980] but, since it is a beta emitter, its measurement is difficult and errors of measurements are high. Attempts to measure it in old falls did not yield any conclusive results [*Bhandari et al.*, 1979].

[12] In this paper we report the ^{44}Ti measurements covering a period of ~235 years (1766 to 2001) based on 19 meteorites, extending the work of *Bonino et al.* [1995], who measured nine meteorites which fell during 1883 to 1993 AD, by another 125 years. Some of the measurements have been made with a much improved system and consequently provides better precision than reported earlier.

5. Selection of Meteorites

[13] Twenty fragments of nineteen ordinary chondrites (H, L, and LL) were selected based on their availability, size, and date of fall to cover the past 235 years. These include some chondrites studied earlier [*Bonino et al.*, 1995, 2001, 2002]. Their source and other details are listed in Table 1. Albareto is the oldest recorded fall measured in this work and was selected because it fell in 1766, just a few decades after the Maunder minimum and the high flux of cosmic rays proposed during this period is expected to have left its record in form of high ^{44}Ti activity. Recent well documented falls like Dhajala (1976), Torino (1986), Mbale (1992), Fermo (1996), and Dergaon (Balidua fragment; 2001), are also included in the present study [*Bhandari et al.*, 1978, 1989; *Murthy et al.*, 1998; *Bonino et al.*, 2001; *Shukla et al.*, 2005].

6. ^{44}Ti Activity in Meteorites

[14] ^{44}Ti is mainly produced in cosmic ray interactions (>70 MeV) in meteoritic iron but there is also some contribution from nickel and titanium. Because of low production cross sections, its activity is extremely low. *Honda and Arnold* [1960] reported ^{44}Ti measurements in two meteorites Bruderheim and Harleton at about 2 and

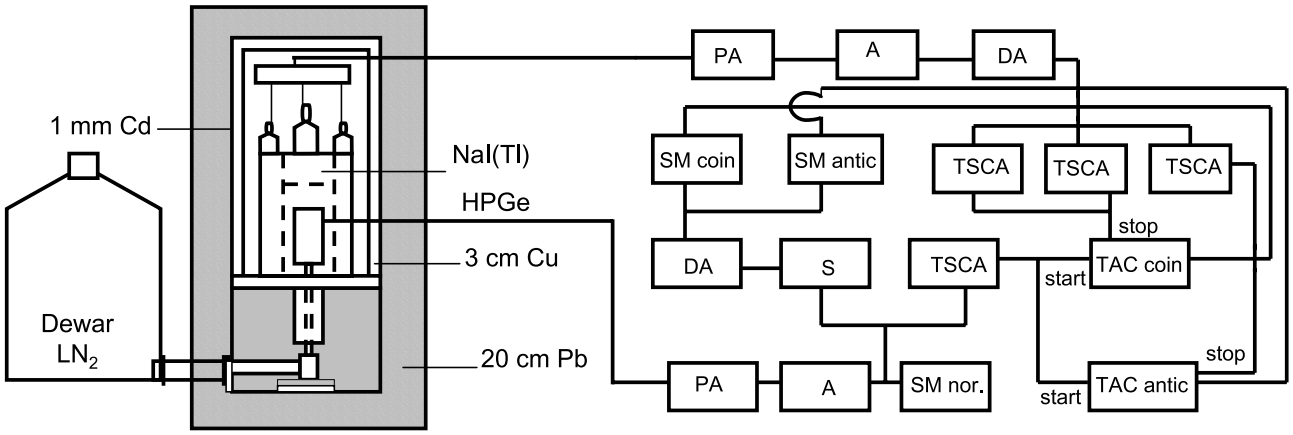

Figure 1. Schematic of the gamma ray spectrometer, lead shield, and the associated electronics used for normal, coincidence, and anticoincidence modes with the NaI (Tl) annulus. For GEM 90, two coincidence channels were used (1) between 1157 keV ^{44}Sc gamma ray and 511 keV line of positron annihilation and (2) 1157 keV and positron annihilation sum peak at 1022 keV for obtaining the coincidence spectra allowing high selectivity, without significant loss of efficiency. For GEM 150, a single channel of coincidence with the positron annihilation sum peak (1022 keV) was used.

1.4 dpm/kg but later attempts by *Cressy* [1964] to systematically measure its activity in several stone and iron meteorites by radiochemical separation in small samples of meteorites did not yield measurable activity.

[15] We have therefore developed a nondestructive gamma ray spectrometric technique, designed specifically for counting ^{44}Ti via its daughter ^{44}Sc. In this spectrometer large samples of meteorites (typically 1 kg) can be counted reliably and with high specificity.

7. Experimental Procedure: Gamma Ray Spectrometer

[16] ^{44}Ti decays to its radioactive daughter, ^{44}Sc ($T_{1/2}$ = 3.93 hours), which emits a positron and a 1157 keV gamma ray in coincidence. A gamma ray coincidence spectrometer, with suitable electronics, tailored to suit the decay scheme of ^{44}Sc, allows a highly sensitive and selective measurement of the positron annihilation lines (511 keV) and their sum peak (1022 keV) emitted in coincidence with the 1157 keV gamma ray. ^{44}Sc (^{44}Ti) could thus be very efficiently counted with this spectrometer and, at the same time, the interference due to the ubiquitous 1155 keV gamma ray from the ambient ^{214}Bi is minimized.

[17] The spectrometer (GEM 90) consists of a principal large (~2 kg, 90% relative efficiency) hyperpure Ge diode operating within an umbrella of a NaI (Tl) scintillator (~28 kg), having a 12 cm diameter cavity in which the Ge detector is located. A rock sample of about 1 kg can be accommodated in this cavity. The Ge detector operates in normal, coincidence, as well as in anticoincidence with the Na(Tl) scintillator. The block diagram of the detectors and the electronics is schematically shown in Figure 1. High counting efficiency and minimum background were attained by adjusting the levels of various modules using a ^{44}Ti source obtained from Argonne National Laboratory, USA. In order to reduce the background further, the system is located in a 20 cm thick low-activity lead shield, having an additional 3 cm thick OFHC copper-Cd-perspex graded shield under the Monte dei Cappuccini in Torino (Italy) having an effective overhead shielding equivalent to 70 m water (m.e.w.). The cavity where the sample is placed is continuously flushed with nitrogen to minimize contribution of the ambient radon and its daughters. The system is described in detail elsewhere [*Bonino et al.*, 1992].

[18] The stability of the counting systems over long counting periods of 10^7 s is within 0.5 keV at energies up to 2 MeV. In order to improve the precision of the measurements further, we have installed a larger Ge detector (GEM 150, ~3 kg with ~150% relative efficiency and resolution of 2 keV at 1332 keV), surrounded by a larger (~90 kg) NaI(Tl) scintillator. Table 2 gives a comparison of the characteristics of the two spectrometers (GEM 90 and GEM 150) used for the measurements reported here. Some of the meteorites earlier counted on GEM 90 were recounted on GEM 150 to improve and confirm the results. The background spectra of GEM 150, obtained in normal, coincidence, and anticoincidence modes, are shown in Figure 2. We note that the ^{214}Bi peak at 1155 keV, which interferes with ^{44}Ti peak at 1157 keV, is nearly eliminated in the coincidence mode. Typical background and efficiency at various energies for GEM 90 and GEM 150 are given in Table 3. It may be noted that background in the 1157 keV peak region, adopted for the ^{44}Ti (^{44}Sc) measurements, is ~0.7 count/day in the coincidence mode.

[19] Using these spectrometers, we have obtained the gamma ray spectra of 19 chondrites, each fragment weighing between 165 and ~1330 g (Table 4). Owing to the low activity, typically a few counts per day, each measurement was carried out for ~10^7 s in order to obtain a reasonable precision. Several peaks due to inherent ^{40}K, U, Th, and cosmogenic radioisotopes could be easily identified in the gamma ray spectra. Small samples for measurements of cosmic ray tracks and potassium analysis were taken, where permitted. We use the normal (or anticoincidence) mode for measurements of ^{40}K and coincidence mode for ^{44}Ti, whereas ^{26}Al could be measured in both normal and coincidence mode. Peaks due to ^{26}Al (1808 keV) and ^{40}K

Table 2. Characteristics of the Two Spectrometers (GEM 90 and GEM 150) Used for the Measurements

	GEM 90	GEM 150
HPGe Detector		
Diameter × height, mm	77.4 × 79.1	91 × 88.4
p-type crystal volume (cm^3)	372	570
^{60}Co γ-radiation at 1332.5 keV		
Relative efficiency	95%	147.1%
Resolution (FWHM)	1.93 keV	1.85 keV
Peak to Compton background ratio:	88	104
^{57}Co γ-radiation at 122 keV		
Resolution (FWHM)	859 eV	871 eV
Crystal surrounding cap	Al, 1 mm	Cu, 1.5 mm
Bias high voltage	2000 V	3700 V
Liquid N_2 dewar capacity	30 l	60 l
NaI(Tl) compound detector		
1. Annular single crystal		
Diameter × thickness, mm	120 × 100	335 × 100
Height, mm	250	300
Annular photomultipliers H.V. bias supply	900 V	900 V
2. Plug single crystal fitting on top,		
H.V. bias supply	1000 V	950 V
Diameter × height, mm	120 × 100	125 × 100
Total detecting volume and mass	7650 cm^3, 28 kg	24900 cm^3, 90 kg
Resolution for ^{137}Cs γ-radiation at 662 keV	8%	10%

(1460 keV) could be easily resolved, whereas ^{44}Ti (1157 keV) peak, due to the contribution from the nearby 1155 keV peak of environmental ^{214}Bi, particularly in the old falls, required optimization by selection of appropriate energy interval for determining the activity.

[20] The spectra, obtained for Dhajala meteorite (fragment 272) in GEM 150, in normal, anticoincidence, and coincidence modes are shown in Figures 2a and 2b and compared with the background spectra given in Figures 2c and 2d. The Mbale, Charsonville, and background spectra in 1157 keV -^{44}Ti peak region are shown in Figure 3 for GEM 90, showing the relative importance of ^{214}Bi peak in older falls. The counting data for various meteorites are given in Table 4.

8. Calculation of ^{44}Ti Activity

[21] The efficiency of counting for various energies was measured in the case of the Torino meteorite by making an identical mould of sediments labeled with known amounts of standard radioisotopes, like ^{109}Cd, ^{139}Ce, ^{57}Co, ^{60}Co, ^{137}Cs, ^{113}Sn, and ^{88}Y. In addition standard ^{26}Al, ^{22}Na (obtained from National Bureau of Standards, USA and New England Nuclear, U.K., respectively), and ^{40}K (KCl) activities were also used to determine the counting efficiencies of the detectors in some specific geometries of counting. This mould and the standards allowed us to construct an efficiency curve as a function of energy for various gamma emitters and positron emitters for the two spectrometers in the three modes of counting (normal, anticoincidence, and coincidence). For all other meteorites, the inherent ^{40}K present in the meteorites was used as an internal standard to correct for the counting geometry of various rocks. The basic assumption in this method is that potassium is uniformly distributed throughout the meteorite. Whereas this assumption is valid for most chondrites and equilibrated achondrites, in some cases like Portales Valley, which is not homogeneous with respect to iron and silicate content, this assumption is not valid. Hence results obtained on Portales Valley [*Bonino et al.*, 2002] are not included in this paper. In view of the importance of potassium concentration in the procedure used for calculating ^{26}Al and ^{44}Ti activities, special emphasis was placed on measurement of potassium concentration with high precision. Wherever possible, potassium was measured in meteorite samples (∼20 g) in a fixed geometry using KCl as a standard. Where we were not permitted to use large samples of meteorites, potassium was determined analytically in representative aliquots (several g) at Joint Research Center at Ispra (Italy) or at Physical Research Laboratory, Ahmedabad (India) using atomic absorption spectrometry. However, in a few cases where we were not permitted to consume any meteorite sample, we use the values reported in literature (e.g., *Kallemeyn et al.* [1989] and compilation of *Mason* [1971]) or the mean value of the particular class of the meteorite. In these cases, there may be additional errors in the calculated activities of ^{44}Ti and ^{26}Al given in Table 5.

[22] To determine the production rate of the ^{44}Ti in meteorites it is necessary (1) to normalize the measured activity to target element (Fe, Ni, and Ti) abundances; since Ti concentration in meteorite is small (few hundred ppm), we only consider Fe and Ni and normalize the measured activity to their concentrations, and (2) to evaluate the effect of shielding depth within the meteoroid. The Fe and Ni abundances have been determined by chemical analysis of meteorite, wherever possible or taken from literature. The errors of measurements of ^{26}Al activity are better than 1%. In case of ^{44}Ti, the errors in fresh falls range between 5 to 15% (1σ), increasing gradually to 20% or larger in old falls (Table 4). Albareto, being the oldest of the measured meteorites (see Table 1), is an exception, where the error of measurement is still larger. Currently, efforts are being made to reduce the errors of measurement using the much improved gamma ray spectrometer (GEM 150) with 2 to 3 times the efficiency and about half the background (Table 2). Remeasurements of Dhajala and Cereseto using GEM 150 confirm the results obtained earlier with GEM 90.

8.1. Half Life of ^{44}Ti

[23] The decay corrections for calculating the ^{44}Ti activity at the time of meteorite fall is sensitive to the half life of the radioisotope. When we started these measurements in 1990,

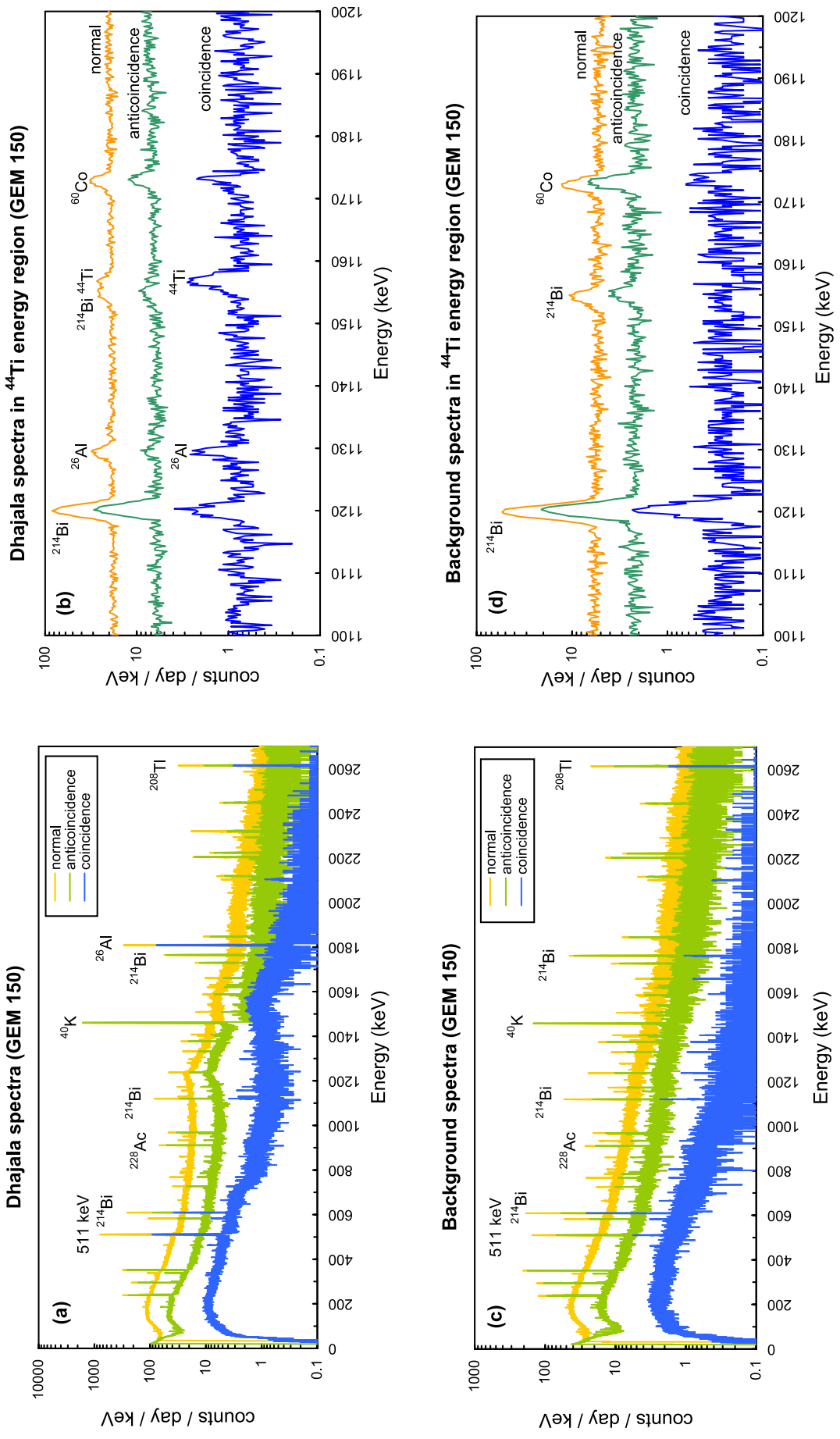

Figure 2. GEM 150-spectra of Dhajala meteorite (72 days) (a) up to 2.7 Mev, (b) 1100 to 1200 keV region containing ^{44}Ti peak and background spectra (91 days), (c) up to 2.7 MeV and, (d) 1100 to 1200 keV region in normal, anticoincidence, and coincidence modes. The typical efficiencies and background rates in various energy regions are given in Table 3.

Table 3. Typical Efficiency (ε in %, for 1 kg Rock) and Gross Background (B, in Counts per Day) of the Gamma Ray Spectrometers in Selected Energy Regions

Mode		^{44}Ti 1157 keV	^{214}Bi 1155 keV	^{40}K 1460 keV	^{26}Al 1808 keV	^{42}Ar 1524 keV
			GEM 90			
Normal	ε	0.87	-	0.8	0.6	0.95
	B	39	78	670	21	12
Coincidence	ε	0.22	-	0	0.15	-
	B	1	1.6	0.7	0.6	0.6
Anticoincidence	ε	-	-	0.8	0.14	-
	B	14	43	470	8	13
			GEM 150			
Normal	ε	2	-	1.5	0.9	0.95
	B	21	48	312	14	16
Coincidence	ε	0.5	-	0	0.44	-
	B	0.7	1.6	0.6	0.5	0.47
Anticoincidence	ε	-	-	1.5	0.2	-
	B	9	19	302	6	8

the half life of ^{44}Ti was not reliably known. A value of 66.6 years obtained by beta counting [*Alburger and Harbottle*, 1990] was used earlier [*Bonino et al.*, 1995]. However, because of various uncertainties in beta counting, it was considered desirable to determine the half life of ^{44}Ti by gamma counting. With this purpose, in a collaborative study, we [*Ahmad et al.*, 1998] have carried out measurements of ^{44}Ti activity in a ^{44}Ti + ^{60}Co source over several years and obtained a value of 59.0 ± 0.6 years. At about the same time *Gorres et al.* [1998] determined the half life value of 60.3 ± 1.3 years. Combining these two precise and more reliable measurements, we obtain a value of 59.2 ± 0.6 years for half life of ^{44}Ti, used here. Subsequently, *Wietfeldt et al.* [1999] have measured a value of 60.7 ± 1.2 years but, since the precision of our measurements is better, we continue to use 59.2 ± 0.6 years. Using this value we have recalculated the activity of ^{44}Ti published earlier [*Bonino et al.*, 1995]. The ^{44}Ti activity of the 19 meteorites at the time of fall is given in Table 5.

8.2. Shielding Correction

[24] The calculations of depth profiles of ^{44}Ti production in bodies of different sizes have been made by *Neumann et al.* [1997] based on the High Energy Transport Code model HETC-HERMES [e.g., *Michel et al.*, 1991, and references therein]. According to these calculations, the ^{44}Ti activity varies between 1.16 and 0.82 dpm/kg meteorite at the surface and 1.18 to 0.4 dpm/kg at the center of meteoroids of different radii (20 to 120 cm), respectively. Thus there can be variation in production rate by a factor of as much as 3, depending on the depth within the meteoroid and its size in the interplanetary space. It is therefore necessary to correct the measured activity for shielding effects due to variations in (r, ΔX) before the activity variations can be attributed to the cosmic ray intensity. In small meteorites of radius <40 cm, however, the production rates are 1.15 ± 0.06 dpm/kg, and the variations are less than 20% implying insignificant shielding corrections.

[25] We have arbitrarily chosen Torino meteorite as a reference representing ''standard'' shielding (meteoroid radius r = 20 cm; depth ΔX = 14 cm) to which we normalize the activity observed in various meteorites. This meteorite was selected simply because it was the first meteorite to be counted in our laboratory. Effectively, using the production profiles of *Michel and Neumann* [1998], we correct the observed activity of ^{44}Ti in each meteorite as if it had the same (r, ΔX) as Torino.

[26] In order to correct for the shielding effects, we have estimated (r, Δx) for each meteorite. This was determined using track density and ^{26}Al data in each meteorite fragment. Track production rates are very sensitive to depth of the sample and to a lesser extent to the size of the meteoroid, particularly if it was a large body in space. We therefore measured the cosmic ray heavy-nuclei track density in mineral grains (olivines, pyroxenes, and feldspars) taken from several locations of the meteorite. This was carried out using standard etching procedures [see, e.g., *Bhandari et al.*, 1980]. The measured track density was corrected for the exposure ages (*Schultz and Kruse* [1989] and the updates given by them) to obtain the track production rates (per cm^2 per million years) which, when compared with the calculated production rate profiles [*Bhattacharya et al.*, 1973], yielded (r, ΔX). We have measured track densities in all the 19 meteorites, of which data for six (Dhajala, Torino, Fermo, Dergaon, Rio Negro, and Mbale) have already been published. The track density values and estimated shielding parameters are summarized in Table 6. In case of multiple falls and showers, data on other fragments were also used following the procedure of *Bhandari et al.* [1980]. In some meteorites it was not possible to determine the preatmospheric size, by track studies alone where ablation geometry could not be ascertained. In such cases we have used the ^{26}Al activity to provide further constraints, since the production profile of ^{26}Al in chondrites of various sizes, based on the model of *Michel et al.* [1991] is well established and has been confirmed experimentally [*Bhandari et al.*, 1991; *Leya et al.*, 2000]. Using the preatmospheric sizes and shielding depth based on tracks and ^{26}Al activity, the shielding corrections were calculated from the ^{44}Ti depth profiles in chondrites given by *Michel and Neumann* [1998]. The shielding corrected ^{44}Ti activity given in Table 5 is independent of the size and shielding depth as well as the target element abundances. It may be noted that, except in

Table 4. Measured Counting Rates in Channels of Interest for 1157 keV ^{44}Ti (^{44}Sc), 1460 keV ^{40} K, and 1808 keV ^{26}Al[a]

	Meteorite	Wt. of Sample Counted, g	Counting Period	Counting Time, days	^{44}Ti (C) Counting Rate per Day (1157 keV)	^{26}Al (N) Counting Rate per Min (1808 keV)	^{40}K (N) cpm (1460 keV)	Decay Time, years
1a	Albareto	605	17.1.1996	225.76	0.34	0.318	1.378	230
			23.9.1996		± 0.11	+ 0.001	± 0.002	
1b	Albareto	560	6.6.2005	79	1.0	0.42	1.9	239
	(GEM150)		24.8.2005		± 0.2	± 0.005	± 0.004	
2	Mooresfort	1145	22.5.2000	362.11	0.79	0.4717	2.1775	189.75
			29.5.2001		± 0.10	± 0.0016	± 0.0099	
3	Charsonville	524	22.1.2002	132.44	0.58	0.3998	1.7099	191.25
			1.6.2002		± 0.14	± 0.0016	± 0.0035	
4	Agen	683	3.12.2002	79.74	0.75	0.3989	1.8948	188.25
			27.3.2003		± 0.18	± 0.0026	± 0.0043	
5	Cereseto	1308	4.7.1995	107.93	1.59	0.5961	2.158	155.25
			11.1.1996		± 0.22	± .0016	± 0.005	
5b	Cereseto	1308	18.8.2003	107.6	2.45	0.82	3.22	163.1
	(GEM 150)		2.12.2003		± 0.4	± 0.0024	± 0.01	
6	Grüneberg	717	24.10.1997	242	0.84	0.36	1.477	156.92
			23.6.1998		± 0.17	± 0.0017	± 0.0038	
7	Kernouve'	820	20.5.1997	154	1.15	0.3492	1.643	128.2
			21.10.1997		± 0.22	± 0.0018	± 0.004	
9	Alfianello	625	11.9.1992	142.35	1.15	0.3724	1.4838	109.76
			2.2.1993		± 0.2	± 0.0015	± 0.0036	
10	Bath	539	29.5.2001	210.55	1.15	0.3675	1.4498	108.75
			22.1.2002		± 0.2	± 0.0012	± 0.0027	
11	Lancon	1080	28.3.1994	100.12	1.9	0.4815	2.019	97.125
			8.7.1994		± 0.3	± 0.0022	± 0.0048	
13	Holbrook	331	2.7.1993	139.47	0.87	0.3129	1.047	81.15
			23.11.1993		± 0.20	± 0.0014	± 0.003	
14	Olivenza	247	18.2.1993	122.81	1.08	0.1968	0.8899	68.84
			22.6.1993		± 0.2	± 0.0012	± 0.003	
15	Rio Negro	388	29.5.1992	89.27	2.09	0.3309	1.295	57.82
			8.9.1992		± 0.3	± 0.0017	± 0.004	
16	Monze	165	29.11.1993	113.13	1.33	0.1380	0.7106	43.28
			2.3.1994		± 0.2	± 0.0085	± 0.0028	
17	Dhajala-272	706	31.7.1990	34	3.14	0.37	1.47	24
			3.9.1990		± 0.73	± 0.003	± 0.0064	
17b	Dhajala-272	706	26.8.2004	71.9	3.74	0.48	2.17	28
	(GEM150)		8.11.2004		± 0.06	± 0.002	± 0.0005	
18	Torino – Aeritalia	445	Jan – March 1991	43.02	3.62	0.2936	1.0621	2.735
					± 0.48	± 0.0035	± 0.0077	
19[a]	Mbale-A	700	2.12.1994	108.37	3.46	0.437	1.8195	2.29
			21.3.1995		± 0.4	± 0.002	± 0.0044	
19b	Mbale-T	730	12.7.1994	117.14	2.91	0.536	1.871	1.9
			22.11.1994		± 0.4	± 0.002	± 0.0041	
20	Fermo	800	19.10.1996	108.81	4.9	0.487	1.7093	0.066
			6.2.1997		± 0.4	± 0.002	± 0.0041	
21	Dergaon (GEM150)	1330	25.8.2005	10	3.98	0.727	1.38	4.48
			5.9.2005		± 1.4	± 0.001	± 0.01	

[a]N: Normal mode, C: coincidence mode. All measurements were made with GEM90 except where GEM150 is mentioned.

Charsonville, Agen, Kernouve, Olivenza, Monze, and Dhajala, the shielding corrections are small (<15%) and any errors on these corrections do not affect the conclusions drawn below.

[27] In case of Fermo, a core was taken and a detailed depth profile of tracks has been obtained, based on which the preatmospheric size and the shielding depth of the sample counted here has been determined. In case of Dhajala, Torino, Mbale, and Dergaon a detailed study of tracks and other cosmogenic effects in several fragments has been made [*Bagolia et al.*, 1978; *Bhandari et al.*, 1988; *Bonino et al.*, 2001; *Murthy et al.*, 1998; *Shukla et al.*, 2005] in spot samples from the fragment counted for ^{44}Ti and these inferred preatmospheric sizes were used in the present work for estimating the shielding corrections. As a result of the more detailed work on Mbale [*Murthy et al.*, 1998], the shielding correction is now better estimated, leading to slightly different activity of ^{44}Ti compared to the values published earlier [*Bonino et al.*, 1995]. In Kernouve', some crystals of apatite showed fission tracks and Rio Negro has track-rich irradiated grains [*Bhandari et al.*, 1995], but these results, being irrelevant for calculation of shielding depth, will not be discussed here and only cosmic ray tracks are considered for determining the shielding depth.

[28] On the basis of the shielding determined by the track density measurements, we have calculated the preatmospheric masses of the meteoroids and mass ablation during their transit through the Earth's atmosphere. These estimates are given in Table 6. The results show that the mass ablation of these meteoroids are high, ranging between 65 and 99.9%.

[29] The counting rates of ^{40}K, ^{44}Ti, and ^{26}Al are given in Table 4 and the calculated activities in various meteorites are given in Table 5. The activity given in Table 5 for various meteorites has been corrected for shielding based on track data given in Table 6 and 26Al activities given in Table 5, as discussed earlier. Statistical errors of measure-

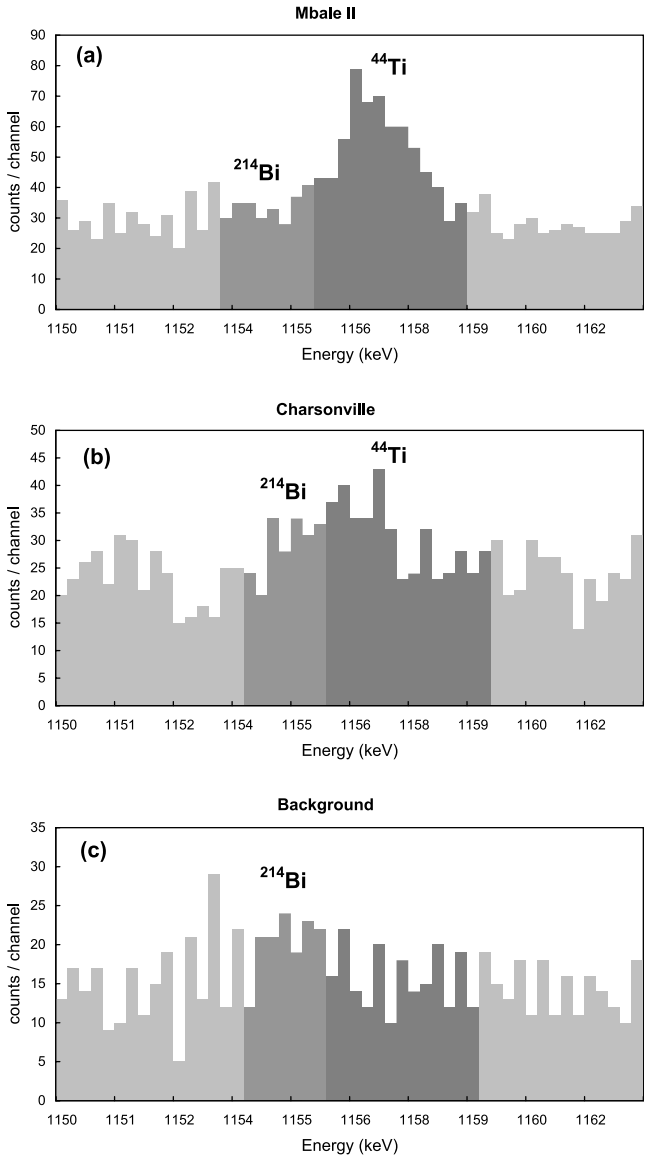

Figure 3. Comparison of the coincidence spectra in the 1150–1200 keV region covering ^{44}Ti (^{44}Sc) 1157 keV and ^{214}Bi interference (at 1155 KeV) in GEM 90 (coincidence mode) for (a) the recent fall Mbale A (1991) for 108 days, (b) the old fall Charsonville (1814) for 132 days, and comparison with (c) the background spectrum for 167 days. The ^{214}Bi and ^{44}Ti regions are marked.

ment (1 σ) are given in these tables. Other sources of errors are due to (1) potassium, iron, and nickel concentrations, estimated to be $\leq$3% in most meteorites, except for Agen and Grüneberg, and (2) shielding correction, which is based on the track and ^{26}Al production profiles [*Bhattacharya et al.*, 1973; *Bhandari et al.*, 1991; *Leya et al.*, 2000] and neon production rates [*Eugster*, 1988] for estimation of exposure ages. These corrections are estimated to be better than ∼5% except for Albareto and Bath.

9. Results and Discussions

[30] The measured ^{44}Ti activity (dpm/kg Fe + Ni), corrected for shielding, is shown in Figure 5 as a function of time of fall of various meteorites. Albareto, Cereseto, and Dhajala were counted on GEM 90 as well as GEM 150. The results are in reasonable agreement, considering the errors of measurements. We use the GEM 150 value for Dhajala and the mean values of the two measurements for the other two meteorites (Albareto and Cereseto) for the following analysis. A linear least squares fit (weighted for errors) through the data on ^{44}Ti activity (dpm/kg meteorite) shows a decreasing trend with time, with some fluctuations (Figure 4a). In Figure 4b, we have also plotted the ^{44}Ti/^{26}Al activity ratio, which varies between a large range of 0.06 and 0.19. We observe a decreasing trend in the ratio; however, the production-depth profiles for the two isotopes being different, as is well known for low-energy (^{26}Al) and high-energy (^{44}Ti) products, the ratio only partially corrects for shielding. In order to perform complete correction for shielding, we apply the procedure described above based on both, the track densities and ^{26}Al activity, obtaining the values of ^{44}Ti activity shown in Figure 5 and Table 5. The ^{44}Ti activity varies by a factor ∼3 between various meteorites (3.7 to 10 dpm/kg Fe + Ni) and the mean for the 19 meteorites is 5.67 dpm/kg (Fe + Ni). A linear least squares fit through the data (Figure 5), shows a decrease of ∼43% during the past 235 years with correlation coefficient of 0.8. In this figure we have excluded Agen because of large errors in ^{44}Ti measurement in this meteorite; in any case, even after excluding Agen, the best fit curve (weighted for errors) remains the same.

[31] Although the time series analysis is limited by the small number of points, in order to determine any trends or periodicities in the data, we use the Singular Spectrum Analysis (SSA) [*Ghil and Taricco*, 1997; *Ghil et al.*, 2002]. For this purpose, we have interpolated the experimental data of Figure 5 at equal sampling interval of Δt = 5 years. We adopt a window width of W = 23 points (corresponding to $W\Delta t \approx$ 115 years), in order to be able to identify any centennial oscillations. The reconstructed components (RCs) 1 to 4 account for ∼84% of the total variance. RCs 1 and 2 correspond to the long-term trend of the series, consistent with the least squares linear fit given in Figure 5. RCs 3 and 4 describe an oscillation with period of ∼87 years similar to the Gleissberg solar cycle. Using this period, suggested by SSA, and taking the errors of measurements into account, we have determined the best fit curve using a straight line and a sinusoid. The analysis thus shows (see Figure 5) a linearly decreasing trend of ∼43% in ^{44}Ti activity during the past 235 years, superimposed on the 87-year oscillation with amplitude (peak to trough) of ∼20%.

10. Comparison With the Calculated Activity of ^{44}Ti: Last 30 Years

[32] Now we compare the measured ^{44}Ti activity in recent falls, e.g., Dhajala, Torino, Mbale, Fermo, and Dergaon, covering the period 1976 to 2001. These meteorites have been studied in detail [*Potdar et al.*, 1986; *Bhandari et al.*, 1989; *Murthy et al.*, 1998; *Bonino et al.*, 2001; *Shukla et al.*, 2005]. The preatmospheric size r and average shielding depth ΔX of the fragments have been determined in all

Table 5. Calculated Activities of ^{44}Ti (Shielding Corrected) and ^{26}Al in Meteorites

Meteorite	^{44}Ti Activity, dpm/kg[a]	(r, ΔX) Based on Tracks, ^{26}Al	Shielding Factor (Torino = 1)	Corrected ^{44}Ti Activity, dpm/kg Fe + Ni	^{26} Al Activity, dpm/kg	^{44}Ti/^{26}Al
Albareto (LL4)	2.33 ± 0.7	40 ± 10,5 ± 2	1.08 ± 0.03	12.0 ± 3.7	53.4 ± 0.2	0.22
(GEM150)	1.55 ± 0.69			(8 ± 3.6)	55.1 ± 0.19	0.15
Mooresfort (H5)	1.75 ± 0.28	50,8	1.13	6.48 ± 1.05	51.2 ± 0.18	0.13
Charsonville (H6)	1.39 ± 0.48	85, 7	1.29	6.4 ± 2.2	48.85 ± 0.19	0.13
Agen (H5)	1.15 ± 0.68	120,15	1.48	8 ± 4.7	43.75 ± 0.29	0.18
Cereseto (H5)	1.65 ± 0.36	50, 8	1.13	6.34 ± 1.4	57.0 ± 0.2	0.11
(GEM 150)	1.55 ± 0.26			5.94 ± 1.0	57.19 ± 0.2	0.1
Grüneberg (H4)	1.48 ± 0.33	75,10	1.22	6.3 ± 1.4	50. 0 ± 0.2	0.13
Kernouve' (H6)	1.39 ± 0.27	120,7	1.45	6.7 ± 1.3	44.7 ± 0.23	0.15
Alfianello (L6)	1.22 ± 0.22	35,10	1.02	5.4 ± 1.0	58.9 ± 0.21	0.09
Bath (H4)	1.25 ± 0.2	50 ± 20,7	1.13	5.1 ± 0.76	52.9 ± 0.18	0.1
Lancon (H6)	1.3 ± 0.2	23,11	1.05	4.85 ± 0.7	49.0 ± 0.50	0.1
Holbrook (L6)	0.8 ± 0.2	40,20	1.13	4.25 ± 1	70.8 ± 0.28	0.06
Olivenza (LL5)	0.9 ± 0.18	85,17	1.41	6.3 ± 1.3	55.1 ± 0.3	0.11
Rio Negro (L4)	1.3 ± 0.2	40,6	1.07	6.0 ± 1.0	56.7 ± 0.27	0.11
Monze (L6)	1.17 ± 0.2	40,20	1.06	5.5 ± 1.0	45.2 ± 0.34	0.12
Dhajala	0.83 ± 0.15	50,16	1.6	4.5 ± 0.82	52.7 ± 0.4	0.09
(Gem 150)	0.82 ± 0.04			4.5 ± 0.2	52.3 ± 0.22	0.09
Torino (H6)	1.2 ± 0.2	20,14	=1	4.24 ± 0.5	51.7 ± 0.36	0.08
Mbale A (L5/6)	1.0 ± 0.1	36,10	1.09	4.7 ± 0.4	60.4 ± 0.3	0.078
Mbale T	0.8 ± 0.1	36,24	1.07	3.7 ± 0.4	72.0 ± 0.3	0.05
Fermo (H3-5)	1.28 ± 0.11	20, 5 ± 3	1	4.15 ± 0.37	57.0 ± 0.3	0.072
Dergaon (H5)	1.07 ± 0.17	20, 7	1.03	3.8 ± 0.6	51.2 ± 0.6	0.072

[a]Not corrected for shielding. All values refer to GEM 90 measurements except where GEM 150 is mentioned.

these meteorites as follows: Torino (r, ΔX) = (20, 14), Fermo (20, 8), Dhajala-272 (50,16), Mbale A (36, 10), Mbale T (36, 24), and Dergaon (20, 7). The measured ^{44}Ti activity in these meteorites is 1.2, 1.28, 0.82,1.0, 0.8, and 1.07 dpm/kg, respectively.

[33] In the Torino meteorite (r, ΔX = 20, 14) the production, Q(r, ΔX) expected from the model of *Michel and Neumann* [1998] is 1.2 dpm/kg meteorite or 4.24 dpm/(kg Fe + Ni), in good agreement with the measured value of 1.15 dpm/kg or 4.2 dpm/(kg Fe + Ni). In the Mbale meteorite, two fragments were counted having shielding

Table 6. Measured Track Densities, Estimated Shielding Depths of Fragments (ΔX) and Preatmospheric Sizes (r) of Various Meteoroids Based on the Observed Track Density

Meteorite	Number of Samples	Exposure Age, M.y.	Track Density Range, cm^{-2}		Ablation (ΔX), cm	(r, ΔX), cm	M_{pre}, kg[a]	Mass Ablation, %
			Olivine	Pyroxene				
Albareto	1	38.9	3.65×10^6	–	5	>15,5	~1000	>99.8
Mooresfort	4	10.3	$2.9–5.9 \times 10^5$	$5.8–11.8 \times 10^5$	8.5 ± 1.5	50,8	1900	99.8
Charsonville	1	63.3	3.03×10^6	–	8 ± 2	>12,8 ± 2	9000	99.7
Agen	3	7	$2–3.75 \times 10^4$	$4.2–8.2 \times 10^4$	12.5 ± 1.5	120,14	26000	99.9
Cereseto	2	4.5	$0.74–1.08 \times 10^5$	$1.5–2.2 \times 10^5$	8–10	40,7	950	99.3
Gruneberg	2	6.7	$1.1–2.8 \times 10^5$	$2.3–5.6 \times 10^5$	0.2–8.4	75,10	6300	99.9
Kernouve'[b]	10	3	$3.46–5.2 \times 10^5$	$6.9–10 \times 10^5$	1.5–4.2	35,10	26000	99.7
Alfianello	1	25.3	1.52×10^5	3×10^5	15.5	35,9	650	64.9
Bath	4	7.4	$1.6–4.4 \times 10^5$	$3.7–7.2 \times 10^5$	2.2–5.2	50 ± 20,7	1900	98.8
Lancon	2	6.6	$1.37,4.56 \times 10^5$	$2.74,9.12 \times 10^5$	6.5–11	23,11	180	96.1
Holbrook	2	16		$0.5,0.8 \times 10^5$	20.5–23	40,20	960	77.1
Olivenza	1	11.6	$<10^5$	-	>15	85,17	9200	98.4
Rio Negro[c]	4	21.5	0.65×10^5–1.64×10^7	1.3×10^5–3.3×10^7	2–17	40,6	950	99.9
Monze	1	9.9	6.9×10^4	1.4×10^5	11	40,12	950	>99.5
Dhajala-272	many	8.9	9.6×10^3	–	24	50,16	1900	96.1
Torino	many	68	3.1×10^5	5×10^5	14 ± 2	20,14	120	99.2
Mbale A	many	26.9	$2.1–3.7 \times 10^5$	$6–1.8 \times 10^5$	12	36,10	700	79
Mbale T	4	8.8	1.6×10^4	3.3×10^4	8–25	36,24		
Fermo	>8	9.7	$0.4–2.7 \times 10^6$	$0.8–5.4 \times 10^6$	2.2–6.2	20,5 ± 3	120	91.5
Dergaon	>4	38.9	$0.8–1.5 \times 10^6$	-	7–9	20,8	120	<91

[a]Considering both track density and ^{26}Al activity (Table 5).
[b]Contains apatites with fission tracks, which have been excluded from the present discussion.
[c]Contains irradiated grains, which have been excluded from the present discussion.

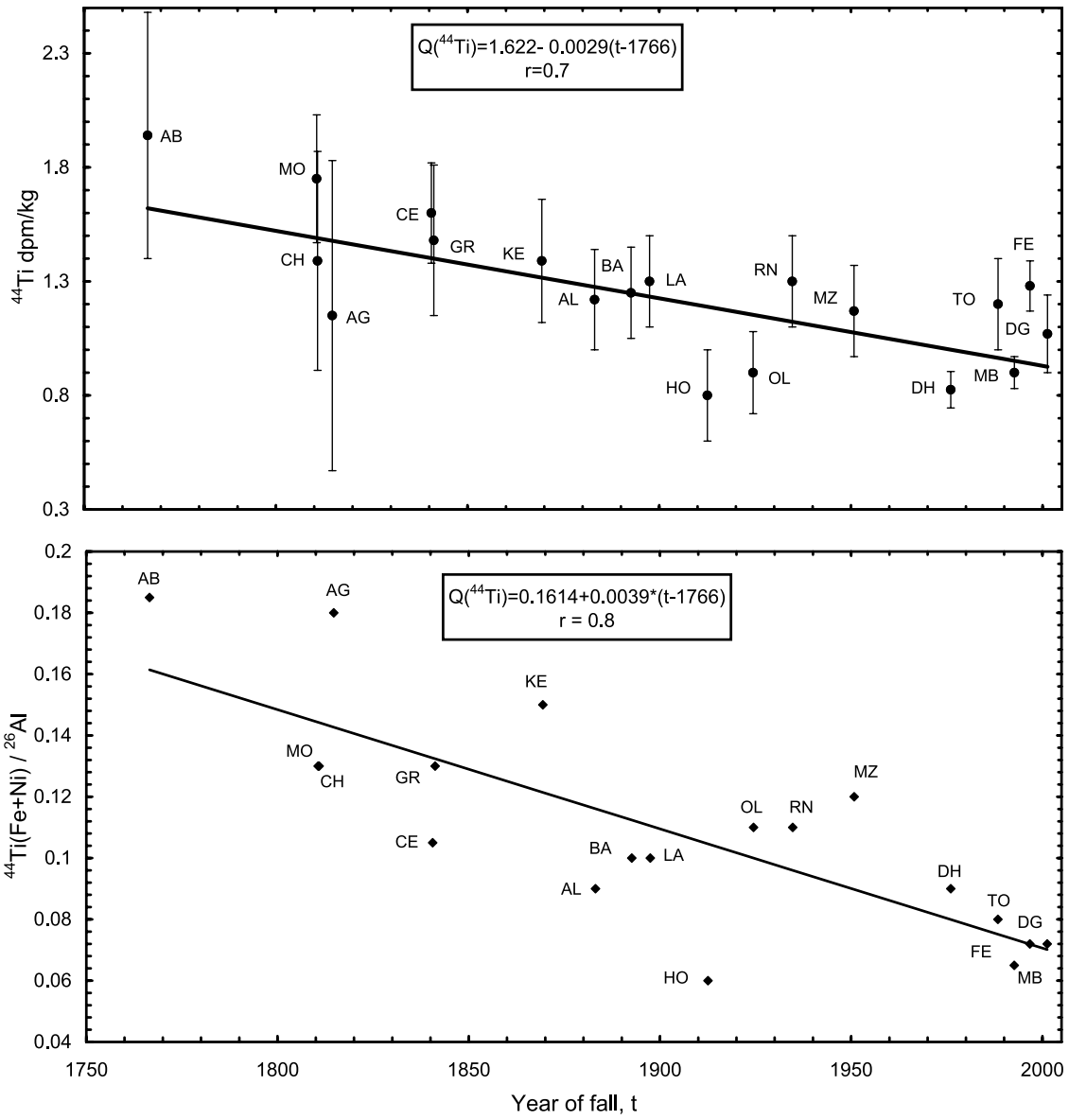

Figure 4. Measured ^{44}Ti dpm/kg (dot) and the composition corrected ^{44}Ti/^{26}Al activity ratio (diamond) as a function of time of fall of meteorites covering the period 1766 to 2001 AD. Albareto (AB), Charsonville (CH), Mooresfort (MO), Agen (AG), Cereseto (CE), Grüneberg (GR), Kernouve' (KE), Alfianello (AL), Bath (BA), Lancon (LA), Holbrook (HO), Olivenza(OL), Rio Negro (RN), Monze (MZ), Dhajala (DH), Torino (TO), Mbale (MB), Fermo (FE), and Dergaon (DG).

depths of ~10 and 24 cm. Both yield approximately the same activity of ^{44}Ti, indicating that there is insignificant change in production rate with depth, consistent with the calculations of *Michel and Neumann* [1998]. We thus find that our measurements in Dhajala, Torino, and Mbale (A and T fragments) are in agreement with the calculations of *Michel and Neumann* [1998] and experimentally validate their production profiles and the GCR flux used by them.

[34] The activity of ^{44}Ti in the five most recent falls covering the period 1976 to 2001, corrected for shielding and chemical composition, is similar within errors, ranging between 3.7 and 4.5 dpm/(kg Fe + Ni) with a mean value of 4.18 dpm/(kg Fe + Ni). This is lower than the mean activity of the meteorites that fell earlier (6.5 dpm/kg Fe + Ni), where the values range between 4.25 and 12 dpm/(kg Fe + Ni), implying that the cosmic ray flux for a period of about 50 years before these recent meteorites fell, during which most of ^{44}Ti was produced, was lower and the solar activity was unusually higher during the present epoch (1976–2001) compared with the past 2 centuries. Similar conclusion has been drawn by *Solanki et al.* [2004] who, based on ^{14}C in tree rings, observe that the level of solar activity during the past 70 years was exceptionally high compared with the past 11,400 years.

11. Comparison With the Calculated Activity of ^{44}Ti: Last 235 Years

[35] The ^{44}Ti activity is proportional to the GCR intensity in space between 1 and about 3 AU [*Gorin et al.*, 2004],

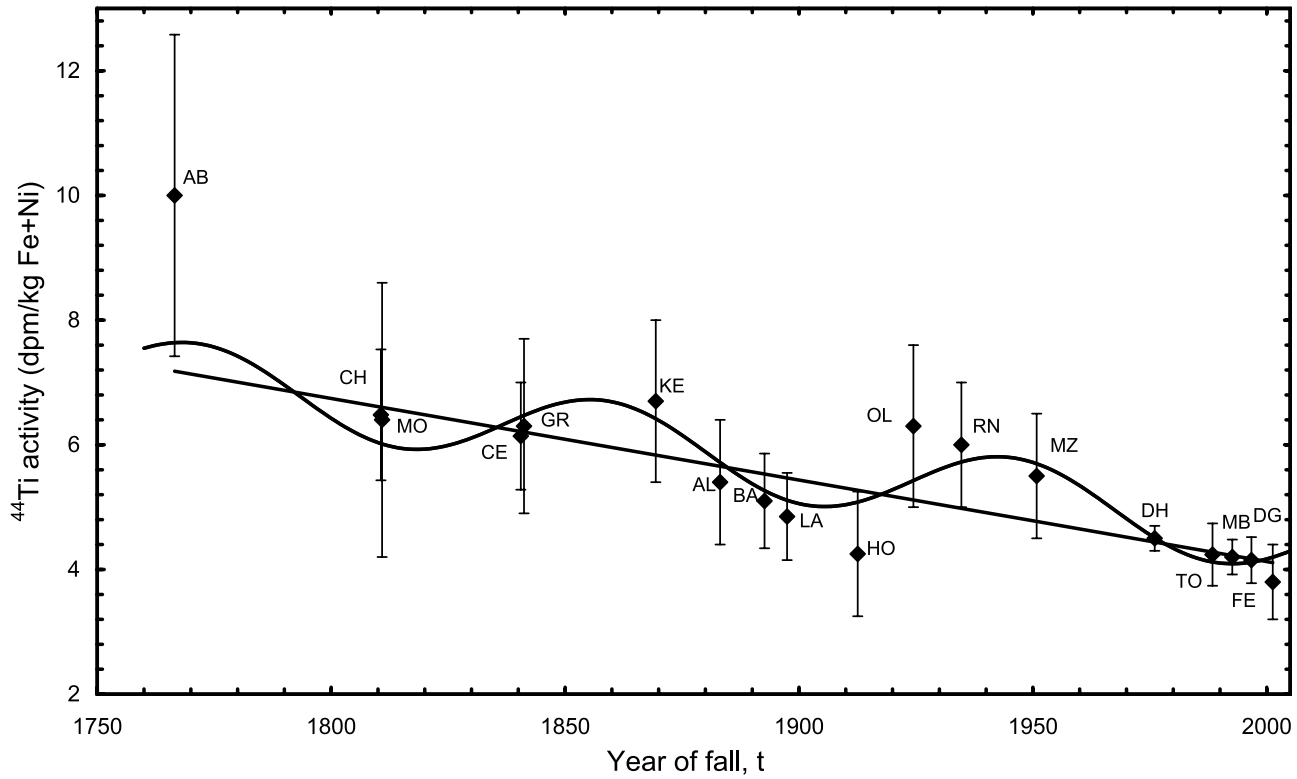

Figure 5. ^{44}Ti activity (dpm/kg Fe + Ni), corrected for shielding and target element composition as a function of time in chondrites: the codes are the same as in Figure 4. The least-square linear trend (y = 30.28 – 0.0131 * t, correlation coefficient = 0.8 and the best fit curve using a straight line and a sinusoid with period of 87 years is superimposed on the data.

where meteorites are exposed to cosmic rays and therefore we use these data to deduce the cosmic ray flux, J_G, during the past 235 years, the period covered by the fall of meteorites, following the procedure discussed below.

[36] Since solar cycle 20, new balloon and spacecraft measurements of cosmic ray energy spectra have been made and 27 spectra are available covering the period 1963–1998 [*Hsieh et al.*, 1971; *Kroeger*, 1986; *Potdar*, 1981; *Cane*, 2003 and references therein]. Using the best fit curves of each of these spectra, following the formulation of *Castagnoli and Lal* [1980], modified using the new interstellar spectra [*Webber and Lockwood*, 2001; *Burger et al.*, 2000], we calculate the values of the modulation parameter Φ for each of these spectra. The calculated J_G values (>70 MeV) agree with the experimental data, indicating that the singular-parameter formulation can be used with confidence to determine J_G. It may be noted that the local interstellar (LIS) flux (>70 MeV) for Φ = 0 for *Castagnoli and Lal* [1980] formulation is about 13 protons/(cm^2 s 4π sr. MeV), whereas *Burger et al.* [2000] give a value of 20.5 p/(cm^2 s 4π sr MeV). This difference arises mainly because of the shape of spectra at high energy (>10 GeV) which is not very effective in isotope production; in the energy region of interest (70 MeV to 10 GeV) both the formulations give similar results.

[37] We use the following relationship for modulated $J_G(T, \Phi)$:

$$J_G(T,\Phi) = J_{LIS}(T+\Phi)\frac{T(T+2T_0)}{(T+\Phi)(T+\Phi+2T_0)} \qquad (1)$$

where $J_{LIS}(T)$ is the unmodulated LIS spectrum, given by *Burger et al.* [2000]:

$$J_{LIS}(T) = 1.9\cdot 10^4 \frac{P(T)^{-2.78}}{\left(1+0.4866\cdot P(T)^{-2.51}\right)}. \qquad (2)$$

T is the kinetic energy of the nucleon, Φ is the modulation parameter, T_0 is the rest energy of the nucleon (938 MeV for protons) and

$$P(T) = \sqrt{T\cdot(T+2T_0)}.$$

We thus obtained Φ values for each of the 27 measured cosmic ray spectra during 1963 to 1998, covering different modulation phases of the three full solar cycles.

[38] Since the ^{44}Ti activity recorded in meteorites depends on the cosmic ray flux, which, in turn, depends on the heliospheric magnetic field, in order to have an independent assessment, we looked for different solar magnetic flux data covering the last 3 centuries. *Solanki et al.* [2000] have reconstructed the open magnetic flux f_0 at the solar surface back to about 1700 AD. A critical point of their work, however, is that they assumed open flux equal to zero at the end of the Maunder minimum. In comparison, *Lockwood* [2003] and *Lockwood et al.* [2004] starting from the open flux observed during the first Ulysses perihelion pass, ran the model backward and obtained the open flux at the end of the Maunder minimum that is about a third of the present day value; they found that this value is consistent

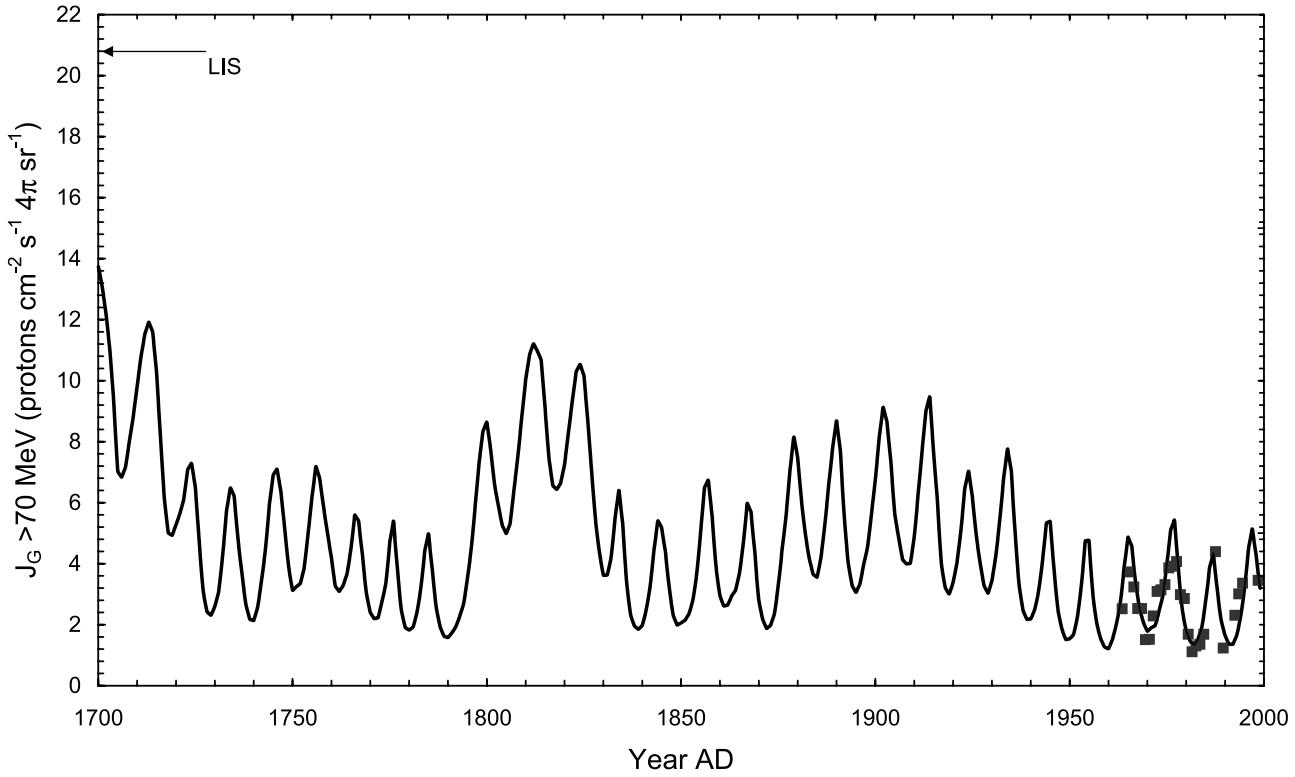

Figure 6. The reconstructed GCR flux J_G (>70 MeV) as a function of time. Solid squares are the values of J_G(t) from the available 27 experimental data sets, discussed in the text. The local interstellar value of J_G (LIS) is shown (arrow) for comparison.

with the ^{10}Be abundances from the Dye-3 Greenland ice core [*Beer et al.*, 1990, 1998]; this is also in agreement with our ^{44}Ti results shown in Figure 6. We also note that the ^{44}Ti decrease since 1900 confirms the long-term drift found in ^{10}Be from Greenland, but not present in ^{10}Be from Antarctica [*Raisbeck et al.*, 1990], probably due to the low accumulation rate on the Antarctic plateau. Moreover, *Lockwood et al.* [2004] have shown that the model of *Solanki et al.* [2000] correctly predicts the open flux seen by Ulysses during both the perihelion passes.

[39] As there is no agreement on a unique value of f_0 at the end of Maunder minimum, we calculate three quadratic fits corresponding to three possible Φ values (50, 100, and 150 MeV) during the Maunder minimum. We prefer a quadratic fit instead of a linear fit between Φ and f_0, because the latter gives unrealistic negative values of Φ during prolonged solar minima (e.g., Dalton and Maunder), whereas a quadratic relation gives positive values.

[40] Thus we obtain, for Φ = 50 MeV during Maunder:

$$\Phi = 4.73\, f_0^2 + 17.08\, f_0 + 72.40 \qquad r^2 = 0.6 \tag{3}$$

for Φ = 100 MeV:

$$\Phi = 4.03\, f_0^2 + 24.22\, f_0 + 97.11 \quad r^2 = 0.7 \tag{4}$$

for Φ = 150 MeV:

$$\Phi = 4.54\, f_0^2 + 14.20\, f_0 + 144.42 \quad r^2 = 0.7 \tag{5}$$

Using these relations, we extended the Φ and the J_G series (using equation (1)) back to 1700 AD. Figure 6 shows the reconstructed J_G (t) flux (>70 MeV) as a function of time taking, e.g., Φ = 50 MeV during Maunder minimum. From this figure, we note a significant increase in J_G during the prolonged solar quiet periods, i.e., following the Maunder minimum, Dalton minimum, and the Modern minimum during which it was higher compared with the values observed during the past 2 decades. Following *Michel and Neumann* [1998], we calculate the relation between the production rate Q and Φ (using power law) and, by extrapolating this fit, we deduce Q at low Φ values. Then the Φ series allows us to calculate Q since 1700 and finally the ^{44}Ti activity,

$$A(t) = \int_{-\infty}^{t} \lambda Q(t') e^{\lambda(t'-t)} dt',$$

as a function of time.

[41] In Figure 7 we compare the measured activity of ^{44}Ti in various meteorites covering the period 1766–2001 (Table 5, Figure 5) with the calculated activities. There is a general agreement between the measured and the estimated activity decrease over the past 2 1/2 centuries based on $f_0(t)$. The centennial variation in the measured series seems to be larger than indicated by the calculated profile. This observation suggests much weakened modulation of GCR during prolonged solar quiet periods. The data shown in Figure 7 suggest that during the Maunder minimum the

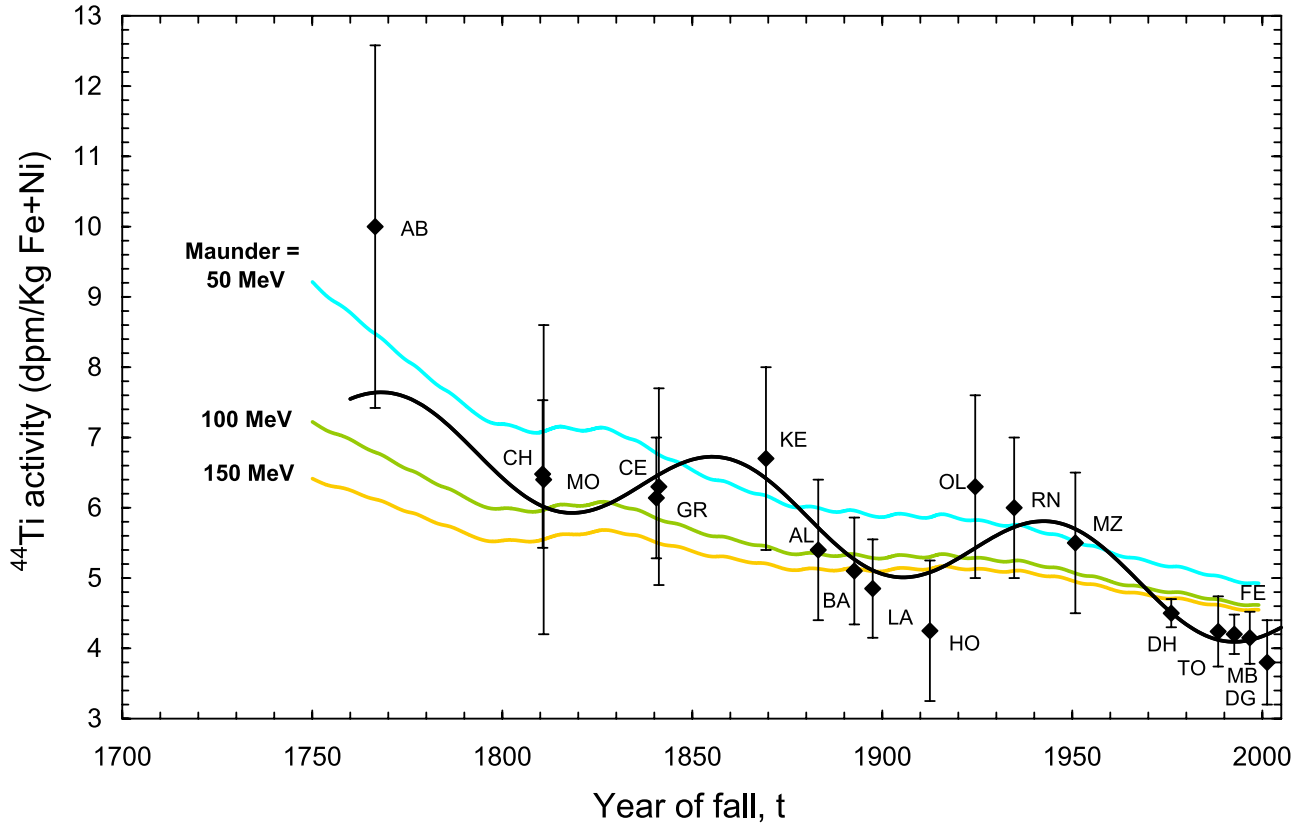

Figure 7. Comparison of the observed ^{44}Ti activity in meteorites (diamond) with the activities expected from Φ(t) series assuming Φ = 50, 100, and 150 MeV during the Maunder minimum (1645–1715) and the production model of *Michel and Neumann* [1998]. The best fit curve through the data, showing a linear decreasing trend and 87 year periodic variation, as in Figure 5, is also shown.

value of Φ was between 50 and 100 MeV, indicating that during this period the flux could have reached ∼65% of LIS.

[42] The consistency between the experimental and the calculated activity is encouraging to use ^{44}Ti as a good proxy of the solar activity over very long periods.

12. Conclusions

[43] The ^{44}Ti activity in the 19 meteorites presented here covers a period of about 235 years between 1766 and 2001 and is related to the century-scale variations of cosmic ray flux in the interplanetary space, where the meteorites are exposed. During this period the solar activity shows, besides the 11-year Schwabe cycle, several epochs of quiet periods, i.e., the Modern, Dalton, Spörer, and Maunder minima. The oldest meteorite studied here fell just when the Sun was recovering from the long-duration (1645–1715) Maunder minimum. Thus with the ^{44}Ti activity profiles shown in Figures 5 and 7, we are able to reconstruct the solar activity from the Maunder minimum to the present epoch and the following conclusions can be made from the data presented here:

[44] 1. The ^{44}Ti activity in meteorites shows a decreasing trend during the past 235 years over which the data are available. This implies that GCR flux in the interplanetary space (1 to 3 AU) has decreased over the past 235 years by about 43%, consistent with the calculated GCR flux in the past based on the evolution of the Sun's large-scale open magnetic field since 1700 [*Solanki et al.*, 2000]. Thus the stony meteorites which fell during the past 3 centuries experienced much higher galactic cosmic ray flux compared to the contemporary flux over the last 3 decades. This is evident by the low activity of ^{44}Ti in the recent falls.

[45] 2. At the end of the Maunder minimum, the increase is consistent with the flux expected from the variation of the long-term evolution of the Sun's large-scale open magnetic field proposed by *Solanki et al.* [2000]. The cosmic ray flux was higher during Maunder minimum and the best agreement with the experimental data is obtained with modulation parameter Φ between 50 and 100 MeV.

[46] 3. The data also indicate that during prolonged quiet periods, like the Gleissberg minima at the beginning of the last 2 centuries, the cosmic ray fluxes were significantly higher. The GCR intensity increase was in the phase expected from sunspot activity but the flux was probably higher than the values computed on the basis of the relationship of solar activity and GCR flux, as also inferred by *Bonino et al.* [1995].

[47] **Acknowledgments.** This paper is dedicated to the memory of our esteemed colleagues G. Cini Castagnoli and Giuseppe Bonino, who contributed significantly but could not complete this study. We thank S. Alessio, A.L. Graham, G.V. Coyne, G. Kurat, P. Pallas, B. Zanda, R.T. Schmitt, H. Betlem, M. Killgore, D. Fontana, E. Galli, and curators of various museums, namely, Vaticano, Berlin, Vienna, Paris, Modena, Torino (Alenia), and Dublin who graciously made the meteorite samples available

for this work. Encouragement and support given by the late Carlo Castagnoli is gratefully acknowledged. We thank A. Romero and K. M. Suthar for careful technical assistance.

[48] Arthur Richmond thanks Michael Lockwood and another reviewer for their assistance in evaluating this paper.

References

Ahluwalia, H. S., and C. Lopate (2001), Long term residual modulation of lower energy galactic cosmic rays, *Proc. Int. Cosmic Ray Conf. XXVII*, 3834–3837.

Ahmad, I., et al. (1998), Three-laboratory measurements of the ^{44}Ti half life, *Phys. Rev. Lett.*, *80*, 2550–2557.

Alburger, D. E., and G. Harbottle (1990), Half lives of Ti-44 and Bi-207, *Phys. Rev. C*, *41*, 2320–2324.

Axford, W. I. (1972), The interaction of the solar wind with the interstellar medium, in *Solar Wind*, edited by C. P. Sonett, P. J. Coleman, and J. M. Wilcox, *NASA Spec. Publ., NASA SP-308*, 598.

Bagolia, C., J. N. Goswami, D. Lal, M. N. Rao, and T. R. Venkatesan (1978), Exposure age and preatmospheric mass of the St. Lawrence chondrite, *Meteoritics*, *13*, 385.

Beer, J., S. Tobias, and N. Weiss (1998), An active Sun throughout the Maunder minimum, *Sol. Phys.*, *181*, 237–249.

Beer, J., et al. (1990), Use of ^{10}Be in polar ice to trace the 11–year cycle of solar activity, *Nature*, *347*, 164–166.

Belov, A. (2000), Large scale modulation: View from the Earth, *Space Sci. Rev.*, *93*, 79–105.

Bhandari, N., S. K. Bhattacharya, and B. L. K. Somayajulu (1978), Cosmogenic radioisotopes in the Dhajala chondrite: Implications to variations of cosmic ray fluxes in the interplanetary space, *Earth Planet. Sci. Lett.*, *40*, 194.

Bhandari, N., H. R. Prabhakara, and R. Raman (1979), Meteorite record of the cosmic rays during the Maunder minimum, *Lunar Planet Sci.* X, *1*, 110–112.

Bhandari, N., D. Lal, R. S. Rajan, J. R. Arnold, K. Marti, and C. B. Moore (1980), Atmospheric ablation in meteorites: A study based on cosmic ray tracks and neon isotopes, *Nucl. Track Detect.*, *4*, 213–262.

Bhandari, N., G. Bonino, E. Callegari, and G. Cini Castagnoli (1988), The Torino meteorite: Classification and cosmogenic effects, *Meteoritics*, *23*, 258.

Bhandari, N., G. Bonino, E. Callegari, G. Cini Castagnoli, K. J. Mathew, J. T. Padia, and G. Queirazza (1989), The Torino H6 meteorite shower, *Meteoritics*, *24*, 29.

Bhandari, N., K. J. Mathew, M. N. Rao, U. Herpers, K. Bremer, S. Vogt, W. Wölfli, H. J. Hofmann, R. Michel, and R. Bodemann (1991), Depth and size dependences of cosmogenic nuclide production rates in meteorides, *Abstr. Annu. Meet. Meteorol. Soc.*, *54*, 20.

Bhandari, N., et al. (1993), Depth and size dependence of cosmogenic nuclide production rates in stony meteoroids, *Geochim. Cosmochim. Acta*, *57*, 2361–2375.

Bhandari, N., G. Bonino, G. Cini Castagnoli, and C. Taricco (1994), The 11 year solar cycle variation of cosmogenic isotope production rates in chondrites, *Meteoritics*, *29*, 443–444.

Bhandari, N., G. Cini Castagnoli, G. Bonino, and K. M. Suthar (1995), Solar flare tracks in Rio Negro (L4) chondrite, *Intl. Cosmic Ray Conf.*, *XXIV*, 1181–1183.

Bhattacharya, S. K., J. N. Goswami, and D. Lal (1973), Semi-empirical rates of formation of cosmic ray tracks in spherical objects exposed in Space: Preatmospheric and post atmospheric depth profiles, *J. Geophys. Res.*, *78*, 8356–8363.

Bieber, J. W., J. Chen, W. H. Matthaeus, C. W. Smith, and M. A. Pomerantz (1993), Long- term variation of interplanetary magnetic field spectra with implications for cosmic ray modulation, *J. Geophys. Res.*, *98*, 3585–3603.

Bonino, G., G. Cini Castagnoli, and N. Bhandari (1992), Measurement of cosmogenic radionuclides in meteorites with a sensitive gamma-ray spectrometer, *Nuovo Cimento C*, *15*, 99–103.

Bonino, G., G. Cini Castagnoli, N. Bhandari, and C. Taricco (1995), Behavior of the heliosphere over prolonged solar quiet periods by ^{44}Ti measurement in meteorites, *Science*, *270*, 1648–1650.

Bonino, G., Cini G. Castagnoli, P. Della Monica, C. Taricco, and N. Bhandari (1997), ^{54}Mn and ^{22}Na in meteorites fell during cycle 22 of solar activity, in *Cosmic Physics in the Years 2000*, *Conf. Proc.*, vol. 58, edited by S. Aiello et al., pp. 295–298, Soc. Ital. di Fis., Bologna, Italy.

Bonino, G., N. Bhandari, S. V. S. Murthy, R. R. Mahajan, K. M. Suthar, A. D. Shukla, P. N. Shukla, G. Cini Castagnoli, and C. Taricco (2001), Solar and galactic cosmic ray records of the Fermo(H) chondrite regolith breccia, *Meteoritics Planet. Sci.*, *36*, 831–839.

Bonino, G., G. Cini Castagnoli, C. Taricco, N. Bhandari, and M. Killgore (2002), Cosmogenic radionuclides in four fragments of the Portales Valley meteorite shower: Influence of different element abundances and shielding, *Adv. Space. Res.*, *29*, 777–782.

Burger, R. A., M. S. Potgieter, and B. Heber (2000), Rigidity dependence of cosmic ray proton latitudinal gradients measured by Ulysses space craft: Implication for the diffusion tensor, *J. Geophys. Res.*, *105*, 27,447–27,456.

Burlaga, L. F., F. B. McDonald, and N. F. Ness (1993), Cosmic ray modulation and the distant heliospheric magnetic field: Voyager 1 and 2 observations from 1986 to 1989, *J. Geophys. Res.*, *98*, 1–11.

Cane, D. (2003), Influence of solar activity variations on the interplanetary space, Ph.D. thesis, 134 pp. Univ. of Turin, Turin, Italy.

Cane, H. V., G. Wibberenz, I. G. Richardson, and T. T. von Rosenvinge (1999), Cosmic ray modulation and the Solar magnetic field, *Geophys. Res. Lett.*, *26*, 565–568.

Castagnoli, G. C., and D. Lal (1980), Solar modulation effects in terrestrial production of carbon-14, *Radiocarbon*, *22*, 133–158.

Castagnoli, G. C., G. Bonino, P. Della Monica, S. Procopio, and C. Taricco (1998), On the solar origin of the 200 yr Suess wiggles: Evidence from thermoluminescence in sea sediments, *Nuovo Cimento C*, *21*, 237–241.

Cohen, T. J., and P. R. Lintz (1974), Long term periodicities in the sunspot cycle, *Nature*, *250*, 398–400.

Cressy, P. J. (1964), Cosmogenic radionuclides in stone meteorites, Ph.D. thesis, Carnegie Inst. of Technol., Pittsburg, Pa.

Damon, P. E., and C. P. Sonett (1991), in *The Sun in Time*, edited by C. P. Sonett, M. S. Giampapa, and M. S. Matthews, p. 360, Univ. of Arizona Press, Tucson, Ariz.

Eugster, O. (1988), Cosmic ray production rate for ^{3}He, ^{21}Ne, ^{36}Ar, ^{83}Kr, ^{126}Xe in chondrites based on ^{81}Kr-Kr exposure ages, *Geochim. Cosmochim. Acta*, *52*, 1649–1662.

Evans, J. C., J. H. Reeves, L. A. Rancitelli, and D. D. Bogard (1982), Cosmogenic nuclides in recently fallen meteorites: Evidence for galactic cosmic ray variation during the period 1967–1978, *J. Geophys. Res.*, *87*, 5577–5591.

Forman, M. A., and O. A. Schaeffer (1980), Ar^{37} and Ar^{39} in meteorites and solar modulation of cosmic rays during the last thousand years, in *The Ancient Sun: Fossil, Record in the Earth, Moon and Meteorites*, pp. 279–292, Elsevier, New York.

Ghil, M., and C. Taricco (1997), Advanced spectral analysis methods, in *Past and Present Variability of the Solar-Terrestrial System: Measurement, Data Analysis and Theoretical Models*, edited by G. Cin Castagnoli and A. Provinzale, pp. 137–159, IOS Press, Amsterdam.

Ghil, M., et al. (2002), Advanced spectral methods for climatic time series, *Rev. Geophys.*, *40*(1), 1003, doi:10.1029/2000RG000092.

Gleissberg, W. (1967), Secularly smoothed data on the minima and maxima of sun spot frequency, *Solar Phys.*, *2*, 231–233.

Gorin, V. D., V. A. Alexeev, and G. K. Ustinova (2004), Preatmospheric sizes and orbits of several chondrites, *Lunar Planet. Sci.*, *25*, 1032–1033.

Gorres, J., et al. (1998), Half-Life of 44Ti as a probe for supernova models, *Phys. Rev. Lett.*, *80*, 2554–2557.

Honda, M., and J. R. Arnold (1960), Effects of cosmic rays on meteorites, *Science*, *143*, 203–212.

Hsieh, K. C., G. M. Mason, and J. A. Simpson (1971), Cosmic ray ^{2}H from satellite measurements, 1965–1969, *Astrophys. J.*, *166*, 221–233.

Jokipii, J. R. (1991), Overview of cosmic-rays, solar and interplanetary physics research, *Rev. Geophys.*, *29*, 907–908.

Kallemeyn, G. W., A. E. Rubin, D. Wang, and J. T. Wasson (1989), Ordinary chondrites: Bulk composition, classification, lithophile element fractionations and petrographic type relationships, *Geochim. Cosmochim Acta*, *53*, 2747–2767.

Kroeger, R. (1986), Measurement of hydrogen and helium isotopes galactic cosmic rays from 1978 to 1984, *Astrophys. J.*, *303*, 816–828.

Lean, J. (2000), Evolution of the Sun's spectral irradiance since the Maunder Minimum, *Geophys. Res. Lett.*, *27*, 2425–2428.

Lean, J. L., Y. M. Wang, and N. R. Sheeley Jr. (2002), The effect of increasing solar activity on the Sun's total and open magnetic flux during multiple cycles: Implications for solar forcing of climate, *Geophys. Res. Lett.*, *29*(24), 2224, doi:10.1029/2002GL015880.

Leya, I., H. J. Langer, S. Neumann, R. Wieler, and R. Michel (2000), The production of cosmogenic nuclides in stony meteoroids by galactic cosmic ray particles, *Meteoritics Planet. Sci.*, *35*, 259–286.

Lockwood, M. (2003), Twenty-three cycles of changing open solar magnetic flux, *J. Geophys. Res.*, *108*(A3), 1128, doi:10.1029/2002JA009431.

Lockwood, M., R. Stamper, and M. N. Wild (1999), A doubling of the Sun's coronal magnetic field during the past 100 years, *Nature*, *399*, 437–439.

Lockwood, M., R. B. Forsyth, A. Balogh, and D. J. McComas (2004), Open solar flux estimates from near-Earth measurements of the interplanetary magnetic field: Comparison of the first two perihelion passes of the Ulysses spacecraft, *Ann. Geophys.*, *22*, 1395–1405.

Masarik, J., and J. Beer (1999), Simulation of particles fluxes and cosmogenic nuclide production in the Earth's atmosphere, *J. Geophys. Res.*, *104*, 12,099–12,111.

Mason, B. (1971), *Handbook of Elemental Abundances in Meteorites*, Gordon and Breach, New York.

Michel, R., and S. Neumann (1998), Interpretation of cosmogenic nuclides in meteorites on the basis of accelerator experiments and physical model calculations, *Earth. Planet. Sci.*, *107*, 207–223.

Michel, R., P. Dragovitsch, G. Dagge, P. Cloth, and D. Filges (1991), On the production of cosmogenic nuclides in extraterrestrial matter by galactic protons, *Meteoritics*, *26*, 221–242.

Murthy, S. V. S., N. Bhandari, K. M. Suthar, C. J. Clement, G. Bonino, and G. C. Castagnoli (1998), Cosmogenic effects in Mbale L 5/6 chondrite, *Meteoritics Planet. Sci.*, *33*, 1311–1316.

Neumann, S., I. Leya, and R. Michel (1997), The influence of solar modulation on short-lived cosmogenic nuclides in meteorites with special emphasis on titanium-44, *Meteoritics*, *32*, A98.

Potdar, M. B. (1981), Nuclear interactions of solar and galactic cosmic rays with interplanetary material, Ph.D. thesis, Gujarat Univ., Ahmedabad, India.

Potdar, M. B., N. Bhandari, and K. M. Suthar (1986), Radionuclide depth profiles in Dhajala chondrite, *Earth Planet. Sci.*, *95*, 169–182.

Potgieter, M. S. (1993), Time-dependent cosmic ray modulation: Role of drifts and interaction regions, *Adv. Space Res.*, *13*, 239–249.

Potgieter, M. S., R. A. Burger, and S. E. S. Ferreira (2001), Modulation of cosmic rays in the heliosphere from solar minima to maxima: A theoretical perspective, *Space. Sci. Rev.*, *97*, 295–307.

Raisbeck, G. M., F. Yiou, J. Jouzel, and J. R. Petit (1990), ^{10}Be and δ^2H in polar ice cores as a probe of the solar variability's influence on climate, *Phil. Trans. R. Soc. London, Ser. A*, *330*, 463–470.

Rouillard, A., and M. Lockwood (2004), Oscillation in the open solar magnetic flux with period 1.68 years: Imprint on galactic cosmic rays and implications for heliospheric shielding, *Ann. Geophys.*, *22*, 4381–4396.

Schultz, L., and H. Kruse (1989), Helium, neon and argon in meteorites: A data compilation, *Meteoritics*, *24*, 155–172.

Shukla, P. N., et al. (2005), The Dergaon, H5 chondrite: Fall, classification, petrological and chemical characteristics, cosmogenic effects and noble gas records, *Meteoritics Planet. Sci.*, *40*, 627–637.

Solanki, S. K., M. Schüssler, and M. Fligge (2000), Evolution of the Sun's large-scale magnetic field since the Maunder Minimum, *Nature*, *408*, 445–447.

Solanki, S. K., I. G. Usoskin, B. Kromer, M. Schüssler, and J. Beer (2004), Unusual activity of the Sun during recent decades compared to the previous 11,000 years, *Nature*, *431*, 1084–1087.

Stozhkov, Y. I., P. E. Pokrevsky, and V. P. Okhlopkov (2000), Long-term negative trend in cosmic ray flux, *J. Geophys. Res.*, *105*, 9–18.

Stozhkov, Y. I., N. S. Svirzhevsky, V. S. Makhmutov, and A. K. Svirzhevskaya (2001), Long term cosmic ray observations in the atmosphere, *Proc. Int. Cosmic Ray Conf. XXVII*, 3883–3886.

Stuiver, M., and P. D. Quay (1980), Changes in atmospheric Carbon-14 attributed to a variable Sun, *Science*, *207*, 11–19.

Urch, I. H., and L. J. Gleason (1972), Galactic cosmic ray modulation from 1965–1970, *Astrophys. Space Sci.*, *17*, 426–446.

Waldmeier, M. (1961), *The Sunspot Activity in the Years 1610–1960*, Swiss Federal Obs., Zurich.

Webber, W. R., and J. A. Lockwood (2001), Voyager and Pioneer space craft measurements of cosmic ray intensities in the outer heliosphere. Toward a new paradigm for understanding the global solar modulation process, 1. Minimum solar modulation (1987 and 1997), *J. Geophys. Res.*, *106*, 29,323–29,331.

Webber, W. R., and S. M. Yushak (1979), The energy spectrum of cosmic ray iron nuclei and the predicted intensity variation during the solar cycle with applications for the intensity observed by a magnetospheric satellite, Final Rep., Air Force Geophys. Lab., Hanscom Air Force Base, Mass.

Wietfeldt, F. E., F. J. Schima, B. M. Coursey, and D. D. Hoppes (1999), Long term measurement of half life of ^{44}Ti, *Phys. Rev C*, *59*, 528–530.

N. Bhandari, Physical Research Laboratory and Basic Sciences Research Institute, Navrangpura, 380009 Ahmedabad, India.

P. Colombetti, D. Cane, C. Taricco, and N. Verma, Dipartimento di Fisica Generale, Università di Torino, Via Pietro Giuria 1, I-10125 Torino, Italy. (taricco@ph.unito.it)